

Surface passivation of InAs(001) with thioacetamide

D. Y. Petrovykh^{a)}

Department of Physics, University of Maryland, College Park, Maryland 20742
and Naval Research Laboratory, Washington, D.C. 20375

J. P. Long and L. J. Whitman^{b)}

Naval Research Laboratory, Washington, D.C. 20375

(Received 29 September 2004; accepted 5 May 2005; published online 9 June 2005)

We describe the passivation of InAs(001) surfaces with thioacetamide (CH_3CSNH_2 or TAM) as an alternative to the standard sulfur passivation using inorganic sulfide $(\text{NH}_4)_2\text{S}_x$. Quantitative comparison using x-ray photoelectron spectroscopy (XPS) demonstrates that TAM passivation dramatically improves the stability against reoxidation in air compared with the inorganic sulfide, with little to no etching during the treatment. We find that TAM passivation preserves the intrinsic surface charge accumulation layer, as directly confirmed with laser-induced photoemission. Overall, TAM appears to provide superior passivation for electronic device and sensing applications. © 2005 American Institute of Physics. [DOI: 10.1063/1.1946182]

The importance of surface passivation for improving the performance of III-V semiconductor devices has been recognized for over a decade.¹⁻³ The features desirable for practical device passivation include the use of wet chemistry, removal of surface oxide and contaminants with minimal substrate etching, and chemical stability of the resulting passivated surface.⁴ A standard ammonium sulfide $[(\text{NH}_4)_2\text{S}_x]$ treatment is widely used to produce S-passivated III-V semiconductor surfaces,² and is therefore a useful benchmark for evaluating other methods.⁴ Effective passivation of GaAs has also been reported with thioacetamide (CH_3CSNH_2 or TAM hereafter).^{5,6} Similarly, on InAs(110), TAM treatment has been reported to produce smaller roughness and more stable tunneling current (during scanning tunneling microscopy) compared to the $(\text{NH}_4)_2\text{S}_x$ passivation.⁷ Here, we compare the two treatments for the technologically important InAs(001) surface in terms of the resulting stability in air and organic solvents and the degree of substrate etching. We also examine the state of the intrinsic surface charge accumulation layer. Overall, we find the TAM passivation to be potentially superior for both electronic device processing and emerging applications in chemical and biological sensing.^{3,4,8}

InAs(001) samples ($\approx 1 \text{ cm}^2$) were diced from a commercial single-side polished undoped wafer (intrinsically n type). The standard TAM solution was prepared by dissolving 0.2 g of TAM powder (ACS reagent grade 99.0%) in 15 mL of dilute NH_4OH (ACS PLUS grade 29.7% $\text{NH}_4\text{OH}:\text{H}_2\text{O}=1:9$ by volume). In contrast to the $(\text{NH}_4)_2\text{S}_x$ passivation,⁴ adding elemental sulfur did not improve the efficiency of the TAM treatment. Samples were degreased in acetone and ethanol for 2 min each, rinsed in triple-distilled water, and dried under a nitrogen flow. Degreased samples were immersed for 4 min in TAM solutions held just below the boiling point ($\approx 78^\circ\text{C}$ waterbath) in loosely capped glass vials. Heated solutions became slightly yellow in color, with a pH of 11.0–11.5 measured with pH paper after the passivation. Following passivation, each sample was rinsed for 2 min in copious amounts of triple-distilled water, dried under

a nitrogen flow, and stored in a covered plastic wafer tray. Three samples were separately prepared and measured 2–3 times each at different time intervals of air exposure.

The passivated surfaces were characterized using x-ray photoelectron spectroscopy (XPS) and laser-induced photoemission spectroscopy (LPS) at room temperature in an ultrahigh vacuum ($<1 \times 10^{-9}$ Torr). Our commercial XPS system is equipped with a monochromatized Al $K\alpha$ source, a magnetic electron lens, and a hemispherical electron energy analyzer (nominal resolution: 0.36 eV for As 3d, In 3d, and 0.9 eV for As 2p; nominal sampled area: Normal emission $<1 \text{ mm}^2$, off-normal angle-resolved data $\approx 150 \times 150 \mu\text{m}^2$).⁹ For XPS data, peak binding energy (BE) and full width at half maximum (FWHM) are reported with 0.1 eV precision.⁹ A home-built LPS setup¹⁰ uses the fifth harmonic of a Nd:YAG laser (5.84 eV) and a double-pass cylindrical mirror electron energy analyzer (0.2 eV nominal CMA resolution, $\approx 40 \times 40 \mu\text{m}^2$ sampled area).

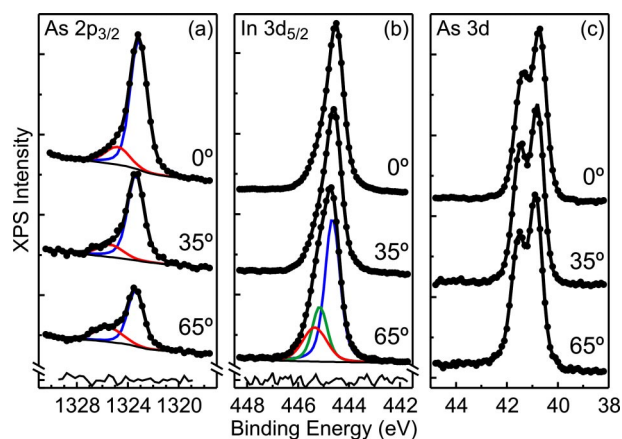


FIG. 1. (Color online) XPS data for TAM-treated InAs(001). After 2 min in water and 5 min in air, As-O_x is only observed in the surface sensitive As $2p_{3/2}$ region (a). Fit parameters: (a) As-In BE=1323.3 eV, FWHM=1.8 eV, As-O_x BE shifts 1.7–2.0 eV, FWHM=2.6 eV, and (b) In-As BE=444.7 eV, FWHM=0.8 eV, In-S BE shift 0.5 eV, FWHM=0.8 eV, In- O_x BE shift 0.7 eV, FWHM=1.2 eV. Full symbols=data; thick lines=fit results; thin lines=fit components and backgrounds; bottom of panels [(a) and (b)]=fit residuals; off-normal emission angles as labeled.

^{a)}Electronic mail: dmitri.petrovykh@nrl.navy.mil

^{b)}Electronic mail: whitman@nrl.navy.mil

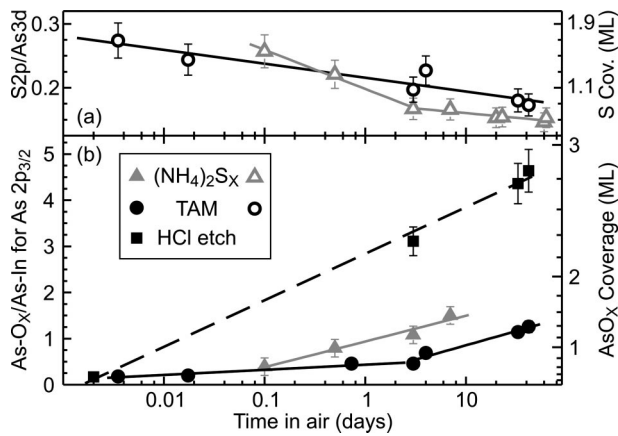


FIG. 2. Stability of S-passivated InAs(001) in laboratory ambient. (a) Comparison of S loss after $(\text{NH}_4)_2\text{S}_x$ and TAM treatment. (b) Reoxidation in air after $(\text{NH}_4)_2\text{S}_x$ and TAM treatment vs an HCl-etched unpassivated control (squares). Gray triangles and lines = $(\text{NH}_4)_2\text{S}_x$ treatment; black circles and lines = TAM treatment. Lines represent semilog fits to data. Right axes indicate corresponding coverages calculated in Ref. 9, where 1 ML = 5.41×10^{14} atoms/cm² for bulk-terminated InAs(001).

We find that the TAM passivation of InAs is remarkably efficient (Fig. 1). A standard evaluation of oxidation and reoxidation of III-V semiconductors is based on measuring characteristic As-O_x features in the As 3d region around 44 eV binding energy.^{4–6,11–13} After TAM passivation, no such As 3d features were observed in normal or off-normal emission [Fig. 1(c)]. Instead, we had to use the more surface sensitive As 2p peaks [Fig. 1(a)] to quantify reoxidation of TAM-passivated surfaces. The attenuation lengths for XPS photoelectrons in InAs are 0.691 nm for As 2p_{3/2} and 3.11 nm for As 3d, thus the As 2p photoelectrons originate almost exclusively in the top few atomic layers.⁹

S-passivated InAs(001) (InAs-S) can be modeled as a stack of alternating In and As crystal planes passivated by a layer of chemisorbed S atoms.^{4,9} This S/In/As “layer-cake” structure is almost exclusively terminated by an In layer with chemisorbed S, which ensures minimal exposure of the topmost As layer to the environment.^{4,9} Some oxidation of the top In layer will be unavoidable in ambient because of imperfections in the S-passivation layer. The small difference between the chemical shifts for In-O_x and In-S makes it difficult to distinguish these In 3d components by XPS.^{4,11,13} For example, in Fig. 1(b), the presence of surface components is indicated by a shoulder which increases in off-normal emission. Fitting and quantitative analysis of the In 3d data are described in detail elsewhere.⁹

Oxidation of As requires breaching the top two layers of the S/In/As layer cake. In combination with the surface sensitivity of As 2p photoelectrons, this requirement makes the As-O_x/As-In intensity ratio a reliable quantitative measure of surface reoxidation after passivation [Fig. 2(b)], which we therefore use to compare TAM passivation to the previous $(\text{NH}_4)_2\text{S}_x$ benchmark.⁴ Quantifying the amount of S on the surface is another way to compare the two passivation treatments [Fig. 2(a)]. Compared to the HCl-etched unpassivated control [squares and dashed line in Fig. 2(b)], both treatments clearly slow reoxidation. There are two reoxidation regimes after TAM passivation: Slow for the first three days (0.11 ± 0.02 slope), and faster (0.62 ± 0.08 slope) for longer air exposures. The latter regime is comparable to reoxidation observed after $(\text{NH}_4)_2\text{S}_x$ passivation (0.56 ± 0.08 slope). The

S coverage data in Fig. 2(a) shows considerably faster S loss for the first three days after $(\text{NH}_4)_2\text{S}_x$ versus TAM passivation (-0.061 ± 0.005 versus -0.021 ± 0.004 slope). No oxidized S species are detected by XPS even after extended exposure to air, indicating the formation of volatile SO_x compounds as the most likely S loss mechanism in both cases. The trends in Figs. 2(a) and 2(b) support a correlation between the stability of the S-passivating layer and robust passivation against reoxidation, as would be expected for a passivating treatment. The S 2p BE = 161.6 eV is essentially identical after both treatments,^{4,9,11,13} so the enhanced stability after the TAM passivation is not due to a dramatic difference in the charge transfer during S chemisorption. The initial S coverages are also similar after both treatments. The enhanced stability of the S layer produced by *organic versus inorganic* sulfide may be related to a difference in adsorbate reactivities, similar to that reported for S-passivation in organic versus inorganic solvents.³

The stability of the TAM-passivated samples was also tested by overnight soaking in common organic solvents: Hexanes, toluene, ethyl acetate, tetrahydrofuran, methylene chloride, and chloroform (all ACS or HPLC grade used without additional purification). The average S coverage after these exposures was reduced by $\approx 15\%$ compared to as-passivated samples. Both stability and oxidation of TAM-passivated samples in solvents were almost identical to the $(\text{NH}_4)_2\text{S}_x$ benchmark, as was the trend of increasing oxidation with decreasing dielectric constant of the solvent.⁴

The etch rate of InAs(001) by TAM solutions proved difficult to measure, because the masking methods used in the $(\text{NH}_4)_2\text{S}_x$ -passivation study⁴ did not withstand the higher temperature and pH of the TAM solutions; specifically, photoresist etch masks became hardened (developed), and poly(methyl methacrylate) masks delaminated. The masking method we found effective was embedding one-half of an InAs sample in freshly cast polydimethylsiloxane (PDMS) followed by hardening the PDMS overnight at room temperature. After 30 min in a concentrated TAM solution, we removed the mask and inspected the samples by optical and atomic force microscopy, but did not observe any etch steps. We thus conclude that the etch rate for InAs(001) in TAM solutions is much slower than the 0.8 nm/min measured in $(\text{NH}_4)_2\text{S}_x$.⁴

The most important electronic property of InAs-S surfaces is the S-induced band bending and the resulting accumulation layer (AL) of conduction-band (CB) electrons.^{4,14} The high-quality of TAM-passivated InAs(001), the narrow band gap of InAs ($E_g = 0.4$ eV), and the use of the spectrally pure 5.84 eV laser excitation enable us to directly observe the CB AL using sensitive low-background LPS. The CB AL appears as nonzero intensity at the Fermi level (E_F) in Fig. 3 (i.e., a significant electron density in CB). The E_F is pinned 0.2 eV above the CB minimum (CBM) confirming that the AL is formed due to S-induced surface band bending, consistent with previous studies of InAs-S.^{4,14} For comparison, in undoped InAs E_F is pinned ≤ 50 meV above the CBM. (Note that only the position and nonzero intensity of the CB peak, but not its shape, are important for the assignment as the CB AL signature.)

The energy scale in Fig. 3 is based on an independent calibration, with E_F determined using a clean Ag surface prior to the measurements, and a standard linear extrapolation of the valence-band (VB) edge placing the VB maxi-

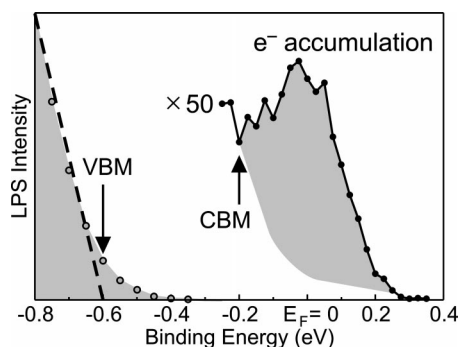


FIG. 3. Electron density at TAM-passivated InAs(001) surface measured by LPS. Positions of the VBM at -0.6 eV and CBM at -0.2 eV are determined from the VB edge (dashed line) and InAs $E_g=0.4$ eV. Nonzero intensity at E_F above the CBM is attributed to an electron accumulation layer at the InAs-S surface (shown scaled up by a factor of 50).

mum (VBM) at -0.6 eV and therefore the CBM at -0.2 eV (offset by E_g). We estimate the CB peak position to be accurate within ≈ 0.1 eV based on the combined uncertainty of the E_F and VBM calibrations. In contrast, the observed width of the CB peak is comparable to the resolution of the cylindrical mirror analyzer and the peak shape is convoluted with a non linear (nearly exponential) background. We note that the high pulsed-laser intensity required to detect the weak CB peak caused an energy shift due to the space charge effect. The shifts measured with relative laser intensities of 2, 1, and $1/3$ were consistent with a linear dependence on intensity,¹⁵ as expected based on a previous systematic LPS calibration for Cu surfaces by one of the authors (J.P.L.). Accordingly, a linear extrapolation of the measurements with neutral density filters to zero intensity was used to correct for the space charge shift.

In conclusion, we have compared TAM and $(\text{NH}_4)_2\text{S}_x$ treatments of InAs(001) and found that TAM solutions provide better surface passivation. High-resolution XPS demonstrates that the TAM treatment is more efficient at removing the native oxide and preventing reoxidation, consistent with the higher stability of the passivating S layer in the resulting S/In/As layer-cake structure.^{4,9} LPS directly confirms the presence of the electron accumulation layer at the TAM-

passivated surface. There are additional practical advantages to using TAM for device passivation, including negligible etching and safer handling. For conventional electronics applications, TAM offers a potentially superior passivation for stabilizing completed devices or for preparing devices for regrowth after processing. For biosensor applications, the organic sulfide solutions closely match those reported for preparation of self-assembled monolayers on GaAs,¹⁶ therefore, the TAM passivation can serve as a benchmark in the development of InAs-based biointerfaces.⁴

One of the authors (D.Y.P.) thanks Dr. Jennifer C. Sullivan for help with the etching experiment. This work was supported by the Office of Naval Research, the Air Force Office of Scientific Research, and DARPA.

¹M. S. Carpenter, M. R. Melloch, M. S. Lundstrom, and S. P. Tobin, Appl. Phys. Lett. **52**, 2157 (1988).

²H. Oigawa, J. F. Fan, Y. Nannichi, H. Sugahara, and M. Oshima, Jpn. J. Appl. Phys., Part 2 **30**, L322 (1991).

³M. V. Lebedev, Prog. Surf. Sci. **70**, 153 (2002).

⁴D. Y. Petrovykh, M. J. Yang, and L. J. Whitman, Surf. Sci. **523**, 231 (2003).

⁵E. D. Lu, F. P. Zhang, S. H. Xu, X. J. Yu, P. S. Xu, Z. F. Han, F. Q. Xu, and X. Y. Zhang, Appl. Phys. Lett. **69**, 2282 (1996).

⁶F. Q. Xu, E. D. Lu, H. B. Pan, C. K. Xie, P. S. Xu, and X. Y. Zhang, Surf. Rev. Lett. **8**, 19 (2001).

⁷L. Canali, J. W. G. Wildoer, O. Kerkhof, and L. P. Kouwenhoven, Appl. Phys. A: Mater. Sci. Process. **66**, S113 (1998).

⁸F. Seker, K. Meeker, T. F. Kuech, and A. B. Ellis, Chem. Rev. (Washington, D.C.) **100**, 2505 (2000).

⁹D. Y. Petrovykh, J. M. Sullivan, and L. J. Whitman, Surf. Interface Anal. (in press 2005).

¹⁰J. P. Long, S. J. Chase, and M. N. Kabler, Phys. Rev. B **64**, 205415 (2001).

¹¹Y. Fukuda, Y. Suzuki, N. Sanada, M. Shimomura, and S. Masuda, Phys. Rev. B **56**, 1084 (1997).

¹²G. Hollinger, R. Skheytabbani, and M. Gendry, Phys. Rev. B **49**, 11159 (1994).

¹³S. Ichikawa, N. Sanada, N. Utsumi, and Y. Fukuda, J. Appl. Phys. **84**, 3658 (1998).

¹⁴M. J. Lowe, T. D. Veal, C. F. McConville, G. R. Bell, S. Tsukamoto, and N. Koguchi, Surf. Sci. **523**, 179 (2003).

¹⁵R. Clauberg and A. Blacha, J. Appl. Phys. **65**, 4095 (1989).

¹⁶T. Baum, S. Ye, and K. Uosaki, Langmuir **15**, 8577 (1999).